A Comparison of Chemical Mechanisms using Tagged Ozone Production Potential (TOPP) Analysis: Supplementary Material

J. Coates[1] and T. Butler[1]

[1]Institute for Advanced Sustainability Studies, Potsdam, Germany

December 3, 2014

S1 Introduction

This is the supplementary material to the research paper "A Comparison of Chemical Mechanisms using Tagged Ozone Production Potential (TOPP) Analysis" and provides further information about the methodology as well as additional analysis.

S2 Mechanism Setup

All chemical mechanisms were adapted into the modularised KPP (Damian et al., 2002) format from their original format for use in the MECCA boxmodel (Sander et al., 2011).

The MCM v3.2 (Jenkin et al., 1997, 2003; Saunders et al., 2003; Bloss et al., 2005; Rickard et al., 2014) was the reference mechanism. Its approach to inorganic chemistry, dry deposition, photolysis and treatment of peroxy radical–peroxy radical reactions were applied to all mechanisms.

S2.1 Photolysis

Photolysis was parameterised as a function of the solar zenith angle as per the MCM approach (Saunders et al., 2003). Mechanism species with a direct MCM v3.2 counterpart were assigned the corresponding MCM v3.2 photolysis rate parameter. Otherwise the mechanism's literature was used to determine the appropriate MCM v3.2 photolysis rate parameter. In some cases this was the MCM v3.2 photolysis rate parameter closest in magnitude to that specified in the mechanism.

For example, in RACM2 the organic nitrate species ONIT has a photolysis rate of 1.96×10^{-6} s^{-1} that was compared to the MCM v3.2 organic nitrate photolysis rate parameters (J_{51} – J_{57}). The rate parameter J_{54} was the most similar and this was assigned as the ONIT photolysis rate parameter in RACM2.

Photolysis of a mechanism species was sometimes represented by more than one MCM v3.2 photolysis reaction. The product yield of the original mechanism reaction was preserved by using a combination of the MCM v3.2 rate parameters. For example, the photolysis of methyl vinyl ketone (MVK) in MOZART-4 is described by the reaction

$$\mathrm{MVK} + \mathrm{h}\nu \longrightarrow 0.7\ \mathrm{CO} + 0.7\ \mathrm{C_3H_6} + 0.3\ \mathrm{CH_3O_2} + 0.3\ \mathrm{CH_3CO_3} \quad \text{(R1)}$$

Whereas in the MCM v3.2 it is described by two reactions

$$\mathrm{MVK} + \mathrm{h}\nu \longrightarrow \mathrm{C_3H_6} + \mathrm{CO} \quad \text{(R2)}$$

$$\mathrm{MVK} + \mathrm{h}\nu \longrightarrow \mathrm{CH_3CO_3} + \mathrm{CO} + \mathrm{HCHO} + \mathrm{HO_2} \quad \text{(R3)}$$

where the photolysis parameters for reactions (R2) and (R3) are designated as J_{23} and J_{24}, respectively. In order to keep the product yield as prescribed in MOZART-4, the photolysis rate parameter assigned to MVK photolysis using the MOZART-4 mechanism is $0.7\ J_{23} + 0.3\ J_{24}$.

S2.2 Organic Peroxy Radical Self and Cross Reactions

Reactions of organic peroxy radicals (RO_2) with other organic peroxy radicals are divided into self ($RO_2 + RO_2$) and cross ($RO_2 + R'O_2$) reactions. These reactions are typically represented in chemical mechanisms as bimolecular reactions which would cause ambiguities when implementing the tagging scheme. Namely, which tag to be used for the products of reactions between RO_2 having different tags. To avoid such ambiguities, the MCM v3.2 approach to self and cross RO_2 reactions is used – all RO_2 react with RO_2 and $R'O_2$ at a single uniform rate. This was represented as a pseudo-unimolecular reaction

Mechanism	**Reaction**	**Rate Constant**
MCM v3.2	C2H5O2 = C2H5O	k*RO2*0.6 s^{-1}
	C2H5O2 = C2H5OH	k*RO2*0.2 s^{-1}
	C2H5O2 = CH3CHO	k*RO2*0.2 s^{-1}
MOZART-4	C2H5O2 + CH3O2 = 0.7 CH2O + 0.8 CH3CHO + HO2 + 0.3 CH3OH + 0.2 C2H5OH	2×10^{-13} cm^3 $molecules^{-1}$ s^{-1}
	C2H5O2 + C2H5O2 = 1.6 CH3CHO + 1.2 HO2 + 0.4 C2H5OH	6.8×10^{-14} cm^3 $molecules^{-1}$ s^{-1}
MOZART-4 modified	C2H5O2 = 0.8 CH3CHO + 0.6 HO2 + 0.2 C2H5OH	2×10^{-13}*RO2 s^{-1}

Table S1: Ethyl peroxy radical ($C_2H_5O_2$) self and cross organic peroxy reactions in the MCM v3.2 and MOZART-4 mechanisms including rate constants. $k = 2(6.6 \times 10^{-27} \exp(365/T))^{\frac{1}{2}}$ $molecules^{-1}$ s^{-1} and RO2 is the sum of all organic peroxy radical mixing ratios.

Reactants	**Products**	**Rate Constant**
MO2 + MO2	0.74 HO2 + 1.37 HCHO + 0.63 MOH	$9.4 \times 10^{-14} \exp(390/T)$ cm^3 $molecules^{-1}$ s^{-1}
MO2	0.37 HO2 + 0.685 HCHO + 0.315 MOH	$9.4 \times 10^{-14} \exp(390/T)$*RO2 s^{-1}
ETHP + MO2	HO2 + 0.75 HCHO + 0.75 ACD + 0.25 MOH + 0.25 EOH	$1.18 \times 10^{-13} \exp(158/T)$ cm^3 $molecules^{-1}$ s^{-1}
ETHP	0.63 HO2 + 0.065 HCHO + 0.75 ACD + 0.25 EOH	$1.18 \times 10^{-13} \exp(158/T)$*RO2 s^{-1}

Table S2: Dermination of ETHP pseudo-unimolecular reaction and rate constant in RACM2 including rate constants. RO2 is the sum of all organic peroxy radical mixing ratios.

whose rate constant includes a factor 'RO2' which was the sum of the mixing ratios of all organic peroxy radicals (Saunders et al., 2003).

The pseudo-unimolecular reaction products and their yields were determined either by using the $RO_2 + RO_2$ reaction and halving the product yields. This is demonstrated for the MOZART-4 treatment of the ethyl peroxy radical in Table S1. Alternatively, the $RO_2 + CH_3O_2$ reaction was used and the products due to CH_3O_2 were removed. Table S2 outlines the steps taken to determine the ETHP pseudo-unimolecular reaction in RACM2.

First the products due to MO2, which represents CH_3O_2 in RACM2, are determined as outlined above using the MO2 + MO2 reaction. The MO2 product yields are then subtracted from the ETHP + MO2 reaction. Any products having a negative yield were not included in the final pseudo-unimolecular reaction.

The methyl acyl peroxy radical ($CH_3C(O)O_2$) was the exception to the above approach. Although most mechanisms include a $CH_3C(O)O_2 + CH_3C(O)O_2$ reaction, its pseudo-unimolecular reaction was derived by subtracting the CH_3O_2 product yields from the $CH_3C(O)O_2 + CH_3O_2$. This approach was used as the $CH_3C(O)O_2 + CH_3O_2$ reaction is the most significant reaction for $CH_3C(O)O_2$.

The rate constant for each pseudo-unimolecular reaction was taken as that of the $RO_2 + CH_3O_2$ reaction multiplied by an 'RO2' factor, which is the sum of the mixing ratios of all organic peroxy radicals. The $RO_2 + CH_3O_2$ rate constant was chosen as this is the most likely reaction to occur in the atmosphere.

S2.3 Dry Deposition

Dry deposition velocities were taken from the MCM v3.2. The dry deposition velocity of MCM v3.2 species of the same chemical functional group was used for mechanism species without direct MCM v3.2 analogues. For example, the dry deposition velocity of PAN species in all mechanisms was equivalent to that of the PAN species in the MCM v3.2.

S2.4 Negative Product Yield Treatment

Some mechanisms include reactions where certain products have a negative yield. These reactions were re-written including an operator species with a positive yield as the analysis tools used in this study does not allow use of negative product yields. The operator species acts as a sink for the original product by immediately reacting with the original product generating a 'NULL' product.

For example, in RADM2 the reaction of cresol (CSL) with OH has negative OH yield (R4).

$$\mathrm{CSL + OH \longrightarrow 0.1\ HO_2 + 0.9\ XO_2 + 0.9\ TCO_3 - 0.9\ OH} \quad \text{(R4)}$$

The negative OH yield was adapted to a positive operator (OHOP) yield (R5) which then immediately reacts with OH giving a 'NULL' product with a rate constant of 8.0×10^{-11} cm^3 s^{-1} (R6). Thus preserving the OH yields using the original mechanism.

$$\mathrm{CSL + OH \longrightarrow 0.1\ HO_2 + 0.9\ XO_2 + 0.9\ TCO_3 + 0.9\ OHOP} \quad \text{(R5)}$$
$$\mathrm{OHOP + OH \longrightarrow NULL} \quad \text{(R6)}$$

S3 Octane O_x Budget Analysis

The RADM2, RACM and RACM2 octane TOPP value time series presented in the paper differ from the MCM v3.2 time series by not reaching their maximum TOPP value on the second day. The attribution of O_x production from octane degradation in MCM v3.2, RADM2, RACM and RACM2 to the number of carbon atoms of the degradation products is depicted in Figure S1.

First day O_x production is similar between the mechanisms. However second day O_x production in RADM2, RACM and RACM2 from octane degradation products having a carbon number between five and three is lower than in MCM v3.2. There is also no O_x production from degradation products having six carbon atoms. Thus octane is broken down so quickly that it cannot reach maximum O_x production on the second day, which is a feature of alkane degradation.

S4 Toluene HO_{2x} Budget Analysis

The paper showed that the CRI v2 maximum daily toluene TOPP value is reached on the second day whilst in the MCM v3.2 this is reached on the first. Figure S2 illustrates the HO_{2x} production budget allocated to the responsible reactions for both the MCM v3.2 and CRI v2. The HO_{2x} production from the reaction of CARB3 and OH in CRI v2 has a larger contribution than its corresponding reaction (GLYOX + OH) in the MCM v3.2.

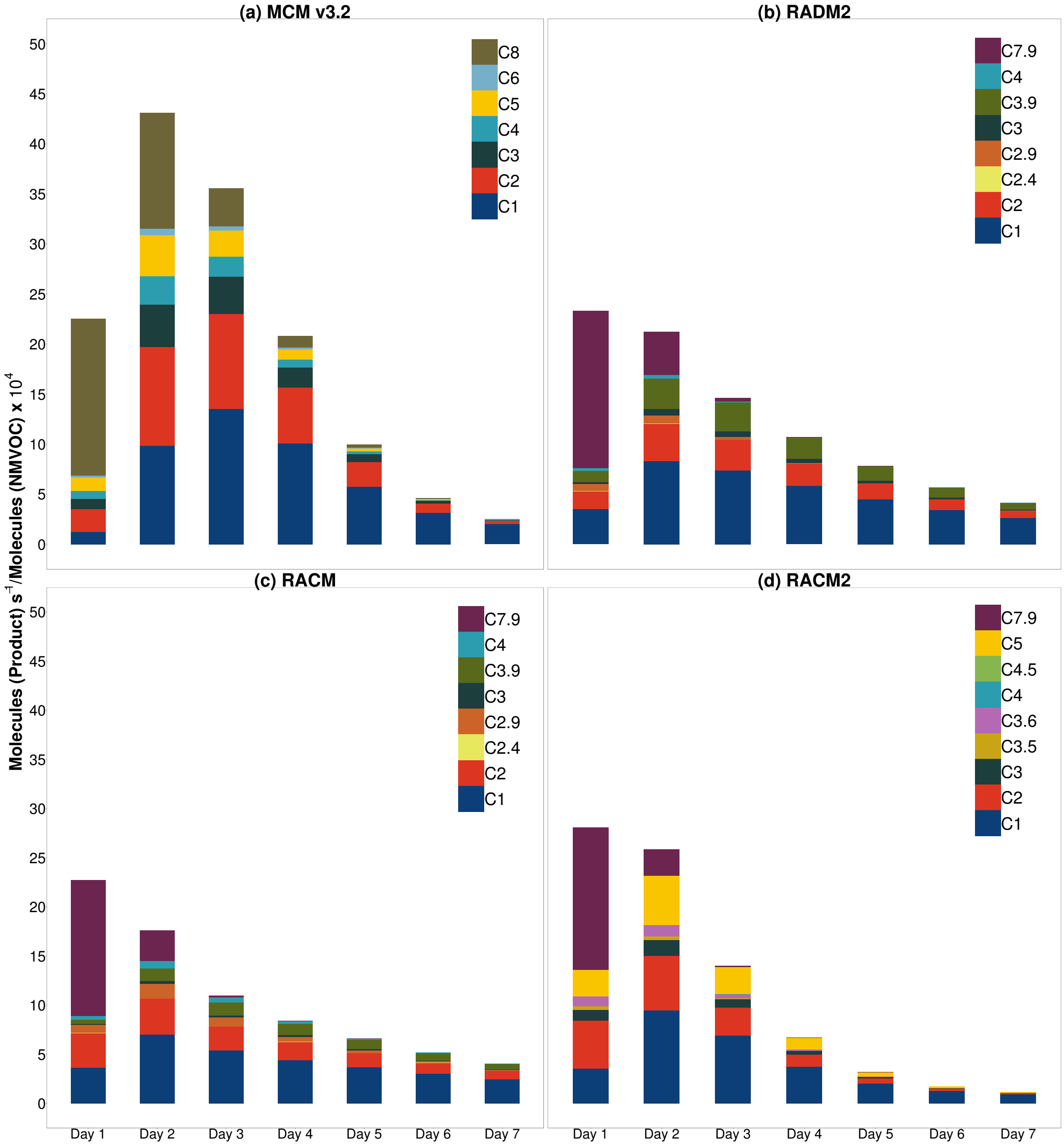

Figure S1: The O_x production budgets from octane degradation attributed to the number of carbon atoms in (a) MCM v3.2, (b) RADM2, (c) RACM and (d) RACM2.

Mechanism	Photolysis Pathway	Rate Parameter
MCM v3.2	GLYOX + hv = CO + CO + H2	J_{31}
	GLYOX + hv = HCHO + CO	J_{32}
	GLYOX + hv = CO + CO + HO2 + HO2	J_{33}
CRI v2	CARB3 + hv = CO + CO + HO2 + HO2	J_{33}

Table S3: Glyoxal photolysis in MCM v3.2 and CRI v2 with specified rate parameters.

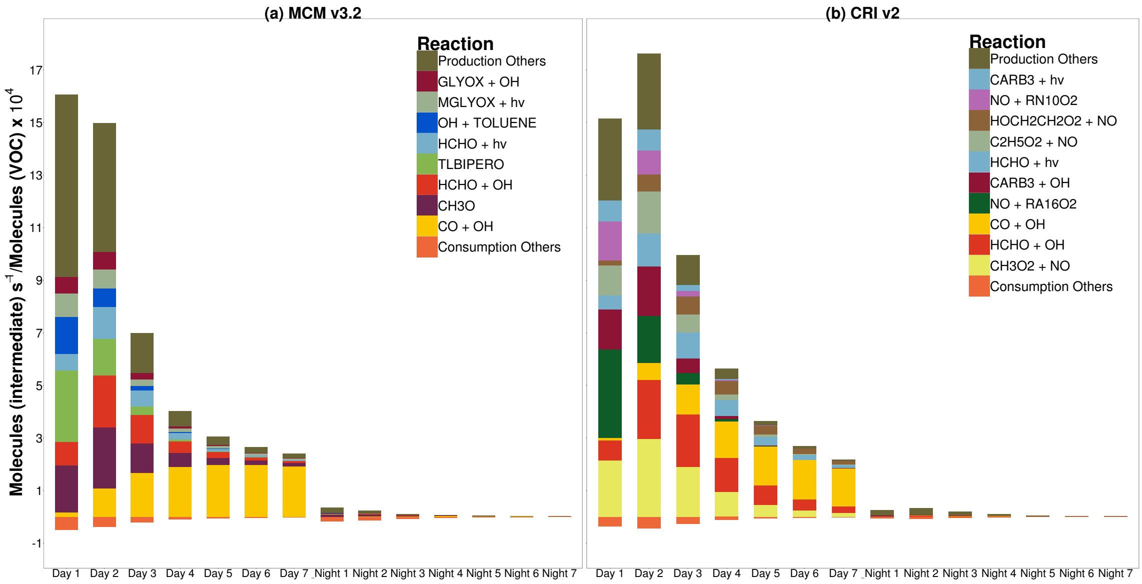

Figure S2: The HO_{2x} production budgets from toluene degradation attributed to the responsible reactions in (a) MCM v3.2 and (b) CRI v2.

Despite glyoxal being represented as CARB3 in CRI v2 and GLYOX in MCM v3.2, there are many differences in how glyoxal chemistry is treated. In CRI v2, CARB3 is only produced from aromatic degradation whilst GLYOX is a degradation product of many other non-aromatic NMVOCs in MCM v3.2.

Glyoxal degradation is through reaction with OH radical and photolysis in CRI v2. Extra degradation options are available in MCM v3.2. Moreover, the rate constant for the reaction with OH radical is $\sim$ 15% faster in CRI v2 than in MCM v3.2.

Glyoxal has three available photolysis pathways in MCM v3.2 and only one in CRI v2. These photolysis pathways and their rate parameters are outlined in Table S3. The additional photolysis pathways in MCM v3.2 are non-HO_{2x} producing pathways leading to less HO_{2x} production.

The combination of the higher rate constant for the glyoxal reaction with OH radical and additional HO_{2x} production during CRI v2 photolysis are responsible for the higher HO_{2x} production in CRI v2.

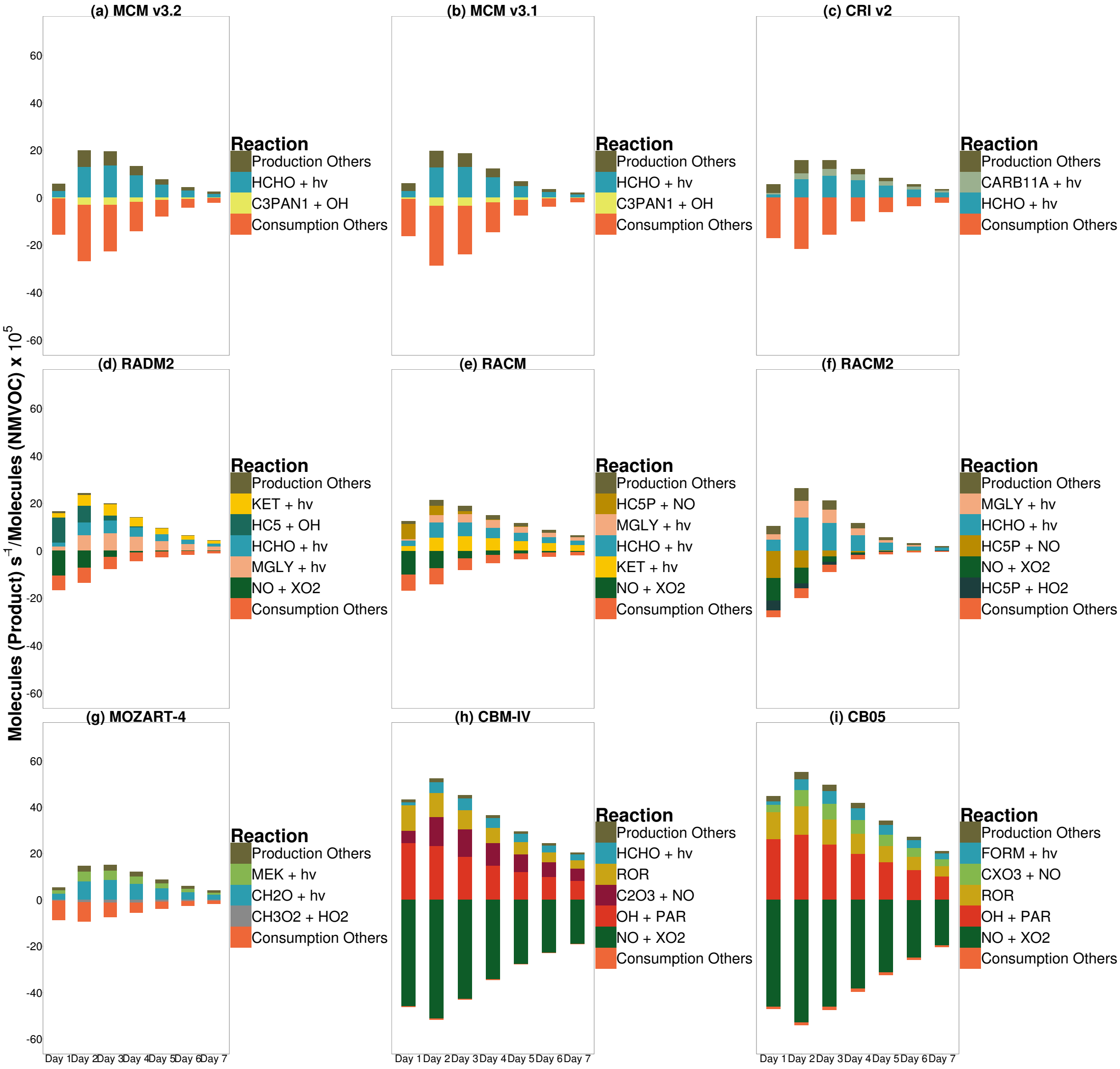

Figure S3: The radical family production and loss budgets from pentane degradation attributed to the responsible reactions in (a) MCM v3.2, (b) MCM v3.1, (c) CRI v2, (d) RADM2, (e) RACM, (f) RACM2, (g) MOZART-4, (h) CBM-IV and (i) CB05.

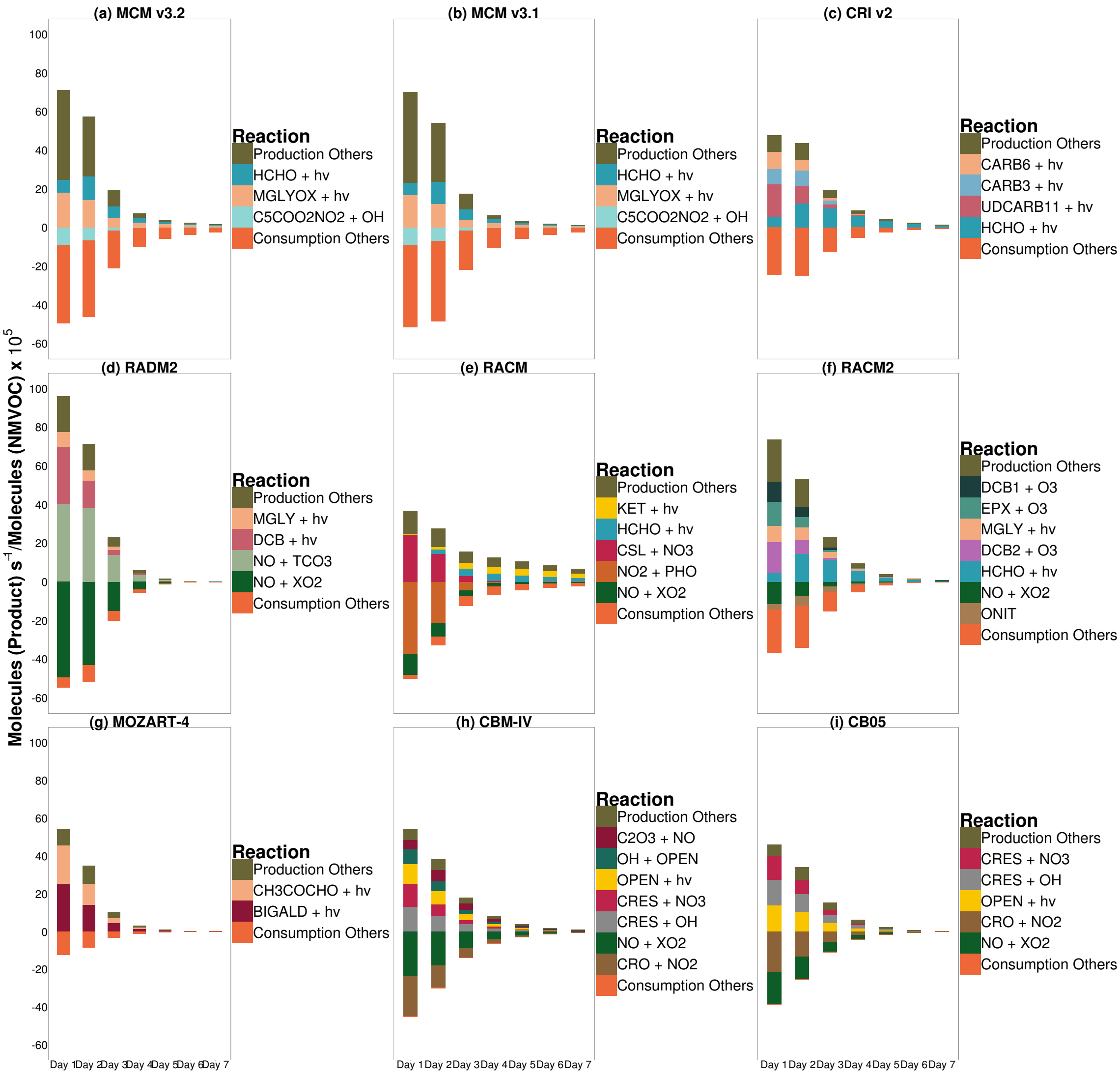

Figure S4: The radical family production and loss budgets from toluene degradation attributed to the responsible reactions in (a) MCM v3.2, (b) MCM v3.1, (c) CRI v2, (d) RADM2, (e) RACM, (f) RACM2, (g) MOZART-4, (h) CBM-IV and (i) CB05.

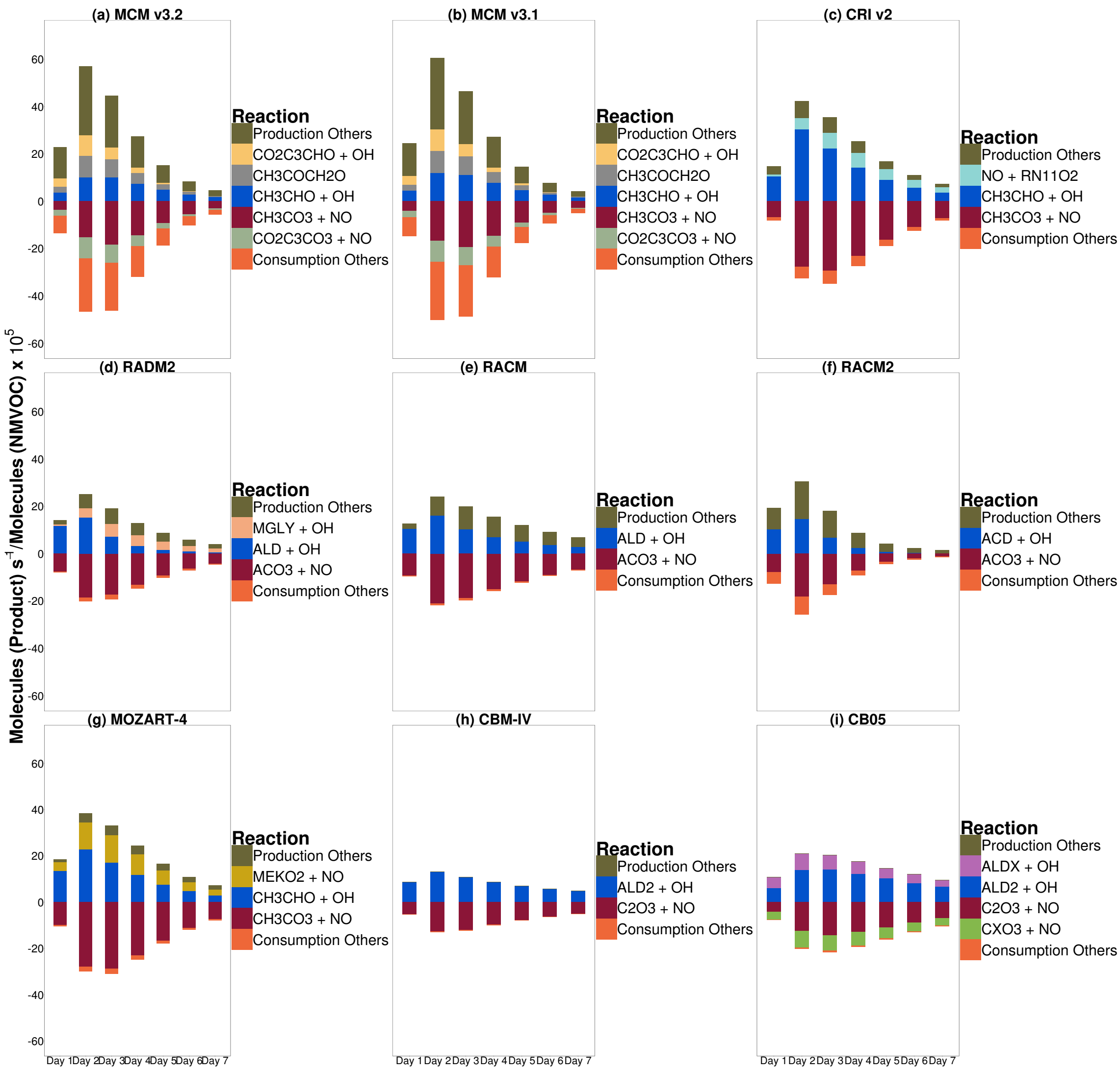

Figure S5: The PAN family production and loss budgets from pentane degradation attributed to the responsible reactions in (a) MCM v3.2, (b) MCM v3.1, (c) CRI v2, (d) RADM2, (e) RACM, (f) RACM2, (g) MOZART-4, (h) CBM-IV and (i) CB05.

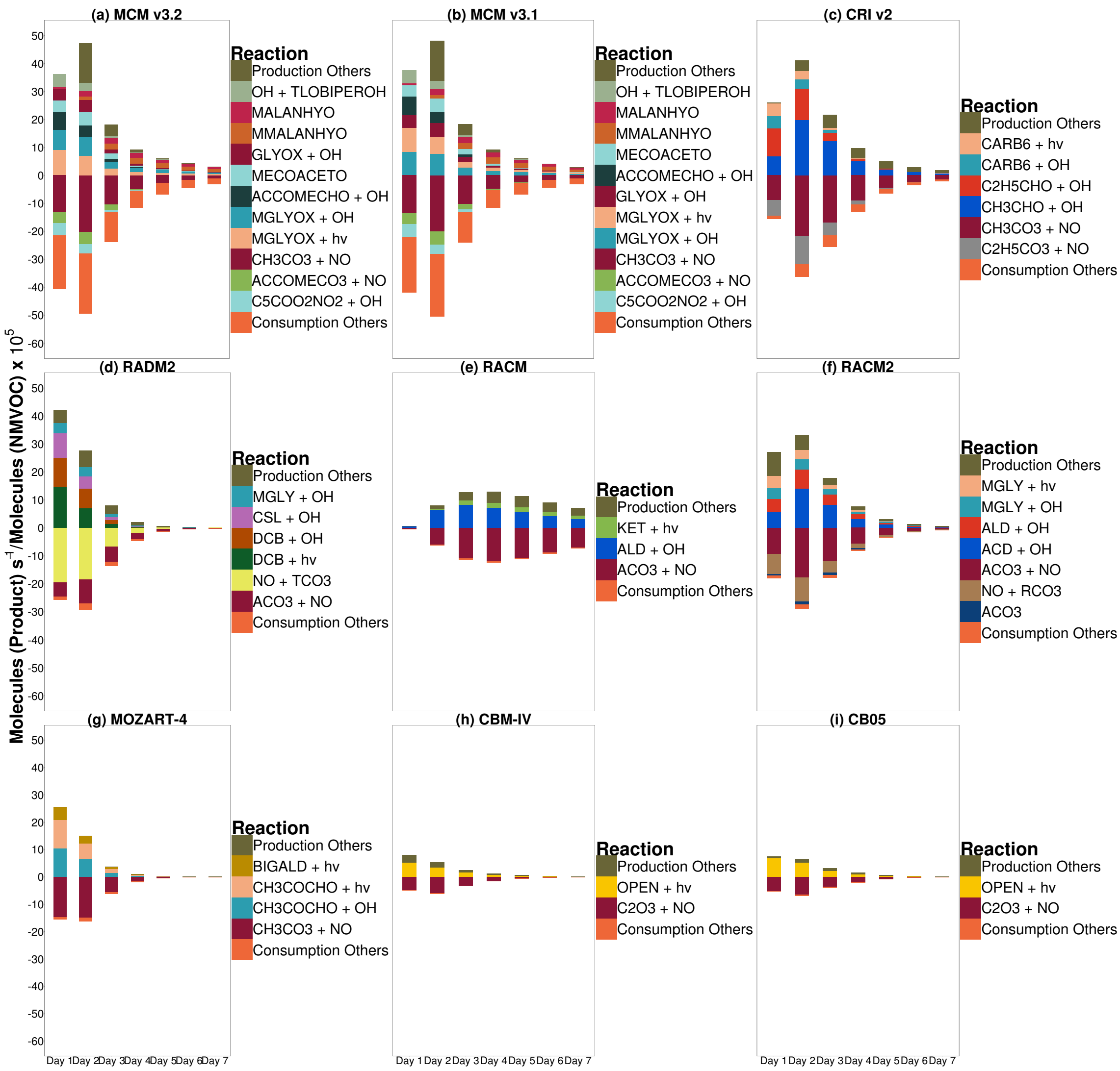

Figure S6: The PAN family production and loss budgets from toluene degradation attributed to the responsible reactions in (a) MCM v3.2, (b) MCM v3.1, (c) CRI v2, (d) RADM2, (e) RACM, (f) RACM2, (g) MOZART-4, (h) CBM-IV and (i) CB05.

S5 Radical and PAN Family Budgets – Additional Plots

In the paper, net radical and PAN family production budgets from alkane, alkene and aromatic degradation was analysed for all mechanisms. As the largest differences were due to alkane and aromatic degradation, the pentane and toluene production and loss budgets from each mechanism was attributed to the responsible processes. These processes are further broken down to the individual reactions.

Figures S3 and S4 depict the reactions contributing to the radical family production and loss budgets of pentane and toluene degradation respectively. Whilst the reactions resposible for PAN family production and consumption are illustrated in Figure S5 and Figure S6.

References

C. Bloss, V. Wagner, M. E. Jenkin, R. Vollamer, W. J. Bloss, J. D. Lee, D. E. Heard, K. Wirtz, M. Martin-Reviejo, G. Rea, J. C. Wenger, and M. J. Pilling. Development of a detailed chemical mechanism (MCMv3.1) for the atmospheric oxidation of aromatic hydrocarbons. *Atmospheric Chemistry and Physics*, 5:641–664, 2005.

V. Damian, A. Sandu, M. Damian, F. Potra, and G.R. Carmichael. The kinetic preprocessor KPP - A software environment for solving chemical kinetics. *Computers and Chemical Engineering*, 26(11):1567–1579, 2002.

M. E. Jenkin, S. M. Saunders, V. Wagner, and M. J. Pilling. Protocol for the development of the Master Chemical Mechanism, MCM v3 (Part B): Tropospheric degradation of aromatic volatile organic compounds. *Atmospheric Chemistry and Physics*, 3(1):181–193, 2003.

Michael E. Jenkin, Sandra M. Saunders, and Michael J. Pilling. The tropospheric degradation of volatile organic compounds: A protocol for mechanism development. *Atmospheric Environment*, 31(1):81–104, 1997.

Andrew Rickard, Jenny Young, and Stephen Pascoe. The Master Chemical Mechanism: Major updates in MCM v3.2. `http://mcm.leeds.ac.uk/MCM/project.htt#New_3.2`, 2014. [Online; accessed 12-November-2014].

R. Sander, A. Baumgaertner, S. Gromov, H. Harder, P. Jöckel, A. Kerkweg, D. Kubistin, E. Regelin, H. Riede, A. Sandu, D. Taraborrelli, H. Tost, and Z.-Q. Xie. The atmospheric chemistry box model CAABA/MECCA-3.0. *Geoscientific Model Development*, 4: 373–380, 2011.

S. M. Saunders, M. E. Jenkin, R. G. Derwent, and M. J. Pilling. Protocol for the development of the Master Chemical Mechanism, MCM v3 (Part A): Tropospheric degradation of non-aromatic volatile organic compounds. *Atmospheric Chemistry and Physics*, 3(1):161–180, 2003.